Electrical modulation of the edge channel transport in topological insulators coupled to ferromagnetic leads

Yuan Li,[1,2,a)] M. B. A. Jalil,[1,3] Seng Ghee Tan,[3] and GuangHui Zhou[4]

[1)] *Department of Electronic and Computer Engineering, Information Storage Materials Laboratory, National University of Singapore, 1 Engineering Drive 3, Singapore 117576, Singapore*

[2)] *Department of Physics, Hangzhou Dianzi University, Hangzhou 310018, P. R. China*

[3)] *Data Storage Institute, DSI Building, 5 Engineering Drive 1 (Off Kent Ridge Crescent), National University of Singapore, Singapore 117608, Singapore*

[4)] *Department of Physics and Key Laboratory for Low-Dimensional Quantum Structures and Manipulation (Ministry of Education), Hunan Normal University, Changsha 410081, China*

(Dated: 26 February 2024)

The counterpropagating edge states of a two-dimensional topological insulator (TI) carry electrons of opposite spins. We investigate the transport properties of edge states in a two-dimensional TI which is contacted to ferromagnetic leads. The application of a side-gate voltage induces a constriction or quantum point contact (QPC) which couples the two edge channels. The transport properties of the system is calculated via the Keldysh nonequilibrium Green's function method. We found that inter-edge spin-flip coupling can significantly enhance (suppress) the charge current when the magnetization of the leads are anti-parallel (parallel) to one another. On the other hand, spin-conserving inter-edge coupling generally reduces the current by backscattering regardless of the magnetization configuration. The charge current and the conductance as a function of the bias voltage, also exhibit similar trends with respect to spin-flip coupling strength, for both parallel and anti-parallel configurations. Hence, gate voltage modulation of edge states via a QPC can provide a means of modulating the spin or charge current flow in TI-based spintronics devices.

PACS numbers: 73.43.-f, 72.25.Dc, 85.75.-d

I. INTRODUCTION

Topological insulators (TIs) are electronic materials that possess an insulating bulk gap and topologically-protected conducting states on their edges or surfaces[1,2]. Bi_2Se_3 and related materials with gapless surface states[3–5], e.g., Bi_2Te_3 and Sb_2Te_3, have recently attracted extensive attention in the condensed matter and device physics communities[6–9]. Thin TI films were proposed for application in the magnetic memory[10] due to their extremely high surface-to-volume ratio[11]. Accordingly, a mechanical exfoliation method was developed for preparation of thin TI films with significant surface transport[12–14].

On the other hand, the two-dimensional version of topological insulators is also known as a quantum spin hall insulator, consisting of edge states that behave as perfect one-dimensional counterpropagating (helical) channels. These channels are well-localized along the edges, carry electrons with opposite spins, and are protected from nonmagnetic impurity scattering by time-reversal symmetry. The peculiar properties of the helical edge states have been demonstrated theoretically and experimentally in HgTe/CdTe quantum wells[15–18], and have been predicted to exist in various other materials[19–24]. Due to the robust spin property of these edge channels, two-dimensional topological insulators are promising candidates for spintronic devices.

In any future spintronic device, it is desirable to achieve electrical (rather than magnetic field) manipulation of spin transport. However, the robustness of the helical edge-state transport to nonmagnetic impurity scattering and local perturbation, means that it is not easy to electrically modulate the edge-state transport in TI-based devices. Nonetheless, investigations into electrical control of edge channel transport in TIs have gathered pace recently. For instance, due to the finite size effect[25], the inter-edge tunneling arising from the overlap between states from opposite edges can open up an energy gap, and modify the conductance of the system. The amplitude of the inter-edge tunneling is determined by the finite decay length of the helical edge states into the bulk[26–30]. This phenomenon may provide a means to adjust the transport property of edge states, via finite size effect of the quantum point contact[31], interferometry of the edge states[32], and nanoscale engineering of the edge geometry, e.g., by patterning a constriction in a HgTe heterostructure[33].

In this article we propose the design of a TI-based spintronics device which incorporates a two-dimensional topological insulator (2D-TI), e.g. a HgTe/CdTe quantum well, contacted to two ferromagnetic leads. We shall focus on the electrical manipulation of the transport properties by inducing inter-edge tunneling through an electrically induced quantum point contact. This can be achieved by applying external voltage via a pair of

[a)] Electronic mail: liyuan@hdu.edu.cn

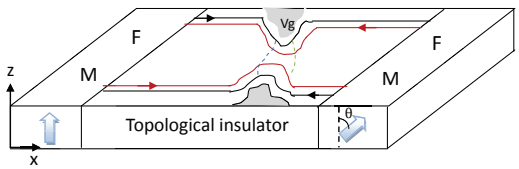

FIG. 1. Schematic description of the proposed two-terminal setup, where edge states flow at the top and bottom boundaries of the topological insulator. There exists a QPC in the central region which can be controlled by the split-gate voltage V_g. Black (red) lines refer to spin-up (spin-down) edge channels, which is assumed to be polarized along the z direction. Application of the split gate voltage V_g reduces the spatial separation of the two edge states, thus increasing the inter-edge tunnel coupling at the QPC region, which is depicted by the blue (green) dashed lines.

split gate along the transverse direction of the device. We apply the nonequilibrium Keldysh Green's function method to calculate the charge current flowing through the TI-based device. It is found that conductance of such device can be significantly enhanced by the presence of inter-edge spin-flip tunneling when the leads are highly spin asymmetric and their magnetizations are in the antiparallel configuration. Thus, the proposed setup can potentially realize an electrically controlled TI device in which the conductance varies according to the inter-edge tunneling coupling and the magnetization configurations of the leads.

The organization of the rest of the paper is as follows. In Sec. II, the Hamiltonian of the system is introduced, and the current formula is derived based on the nonequilibrium Green's function method. In Sec. III, we present the results of our numerical calculation of the charge current and the differential conductance in the presence of inter-edge tunneling couplings modulated by the split-gate voltage. Finally, a brief summary is given in Sec. IV.

II. MODEL AND FORMULA

We consider a TI-based device consisting of a channel made of a 2D-TI bar sandwiched between two ferromagnetic leads [see Fig. 1]. We assume the presence of a gate-bias induced QPC, across which inter-edge coupling occurs. In this paper, we use the low energy effective theory of the edge states to investigate the transport property of the QSH system[32,34]. This system can be described by the following Hamiltonian:

$$H = H_L + H_R + H_C + H_T, \tag{1}$$

where H_C is the effective Hamiltonian describing the QSH edge states

$$H_C = \sum_{\beta k\sigma}(\eta_\beta \eta_\sigma v k) c^\dagger_{\beta k\sigma} c_{\beta k\sigma} + \sum_{k\sigma}[V_{c1} c^\dagger_{tk\sigma} c_{bk\sigma} + \eta_\sigma V_{c2} c^\dagger_{tk\sigma} c_{bk\bar{\sigma}} + c.c.]. \tag{2}$$

In the above, $c^\dagger_{\beta k\sigma}(c_{\beta k\sigma})$ is the creation (annihilation) operator of spin $\sigma =\uparrow (\downarrow)$ for electron constrained along the β edges, where the edge index $\beta = t, b$ refers to the top- and bottom-edge channels. The first term in H_C describes the left- and right-moving QSH edge states, while the second and third terms represent, respectively, the spin-conserving and spin-flip couplings between the two edge channels. Accordingly, v is the edge state velocity, V_{c1} and V_{c2} are, respectively, the spin-conserving and spin-flip tunnel coupling strengths between the edge states. These can be modulated by means of the split-gate voltage V_g which modifies the width of the QPC[32]. The edge and spin states are characterized by the following indexes: $\eta_{t/b} = \pm 1$ and $\eta_{\uparrow/\downarrow} = \pm 1$. In general, in order to preserve time-reverse symmetry, only the two types of coupling represented by V_{c1} and V_{c2} are allowed[2]. In the device operation, an electron is injected from the source electrode and flows through along one of the edges of the topological insulator. An important point to note is that under nonequilibrium condition, the total current is contributed by electrons with different wavevector $\boldsymbol{k}$ corresponding to the conduction "window" between the electrochemical potentials of the source and drain electrodes. However, for simplicity, one can assume the coupling constants to be independent of $\boldsymbol{k}$ and energy over the conduction window (this is especially valid for small source- drain bias).

The Hamiltonian H_L and H_R, which describe the left and right ferromagnetic leads, and H_T which describes the coupling between the FM leads and the central TI region are given by:

$$H_{\alpha=L,R} = \sum_{k\sigma}(\epsilon_{k\alpha} + \eta_\sigma M) a^\dagger_{k\alpha\sigma} a_{k\alpha\sigma} = \sum_{k\sigma} \epsilon_{k\alpha\sigma} a^\dagger_{k\alpha\sigma} a_{k\alpha\sigma}, \tag{3}$$

and

$$H_T = \sum_{k\beta\sigma}\Big[V_{kL,\beta\sigma} a^\dagger_{kL\sigma} c_{\beta k\sigma} + V_{kR,\beta\sigma}(\eta_\sigma \cos\frac{\theta}{2} a^\dagger_{kR\sigma} + \sin\frac{\theta}{2} a^\dagger_{kR\bar{\sigma}}) c_{\beta k\sigma} + c.c.\Big]. \tag{4}$$

$(\epsilon_{k\alpha} + \eta_\sigma M)$ is the energy of conduction electrons in the α lead, and is characterized by the amplitude k of the wave vector, and the amplitude M and orientation η_σ of the magnetization of the FM lead. $a^\dagger_{k\alpha\sigma}$ and $a_{k\alpha\sigma}$ denote the creation and annihilation operators of electrons with spin σ in lead α, while $V_{k\alpha,\beta\sigma}$ denotes the tunnel coupling between the edge state of the TI and the lead.

The charge current can be calculated using the standard Keldysh nonequilibrium Green's function method[35], namely,

$$J_\alpha = \frac{ie}{\hbar}\int \frac{d\epsilon}{2\pi}\mathrm{Tr}\{\mathbf{\Gamma}_\alpha[\mathbf{G}^<(\epsilon) + f_\alpha(\epsilon)(\mathbf{G}^r(\epsilon) - \mathbf{G}^a(\epsilon))]\}, \tag{5}$$

where $f_\alpha(\epsilon) = \{\exp[(\epsilon - \mu_\alpha)/k_B T] + 1\}^{-1}$ is the Fermi-distribution function, and the trace is over both the spin and edge-state indexes. The linewidth $\mathbf{\Gamma}_\alpha(\epsilon)$ is represented by a (4×4) matrix in spin space and edge-state space, which can be written as

$$\mathbf{\Gamma}_\alpha(\epsilon) = \begin{pmatrix} \mathbf{\Gamma}^t_\alpha & \mathbf{0} \\ \mathbf{0} & \mathbf{\Gamma}^b_\alpha \end{pmatrix}, \quad \mathbf{\Gamma}^\beta_\alpha = U^\dagger_\alpha \begin{pmatrix} \Gamma^\beta_{\alpha\uparrow} & 0 \\ 0 & \Gamma^\beta_{\alpha\downarrow} \end{pmatrix} U_\alpha,$$

with

$$U_\alpha = \begin{pmatrix} \cos(\theta_\alpha/2) & \sin(\theta_\alpha/2) \\ -\sin(\theta_\alpha/2) & \cos(\theta_\alpha/2) \end{pmatrix}.$$

Here, θ_α denotes the magnetization direction in lead α, so that we have $\theta_L = 0$ and $\theta_R = \theta$, i.e., fixed (variable) magnetization orientation for lead $\alpha = L$ (R). The components of the linewidth matrix are related to the tunnel couplings as follows: $\Gamma^\beta_{\alpha\sigma}(\epsilon) = 2\pi\sum_k |V_{k\alpha,\beta\sigma}|^2\delta(\epsilon - \varepsilon_{k\alpha\sigma})$. In the following numerical calculation, we assume $\Gamma^\beta_{\alpha\uparrow/\downarrow}(\epsilon) = \Gamma^\beta_{\alpha\uparrow/\downarrow}\theta(D - |\epsilon|)$ and $\Gamma^\beta_{\alpha\uparrow/\downarrow} = \xi_\alpha\Gamma_0(1 \pm p_\alpha)$, where $D = 500$ is the bandwidth, $\Gamma_0 = 1$ is the unit of energy, p_α denotes the spin asymmetry factor for tunneling across the barrier, and ξ_α is the asymmetry in the TI-lead coupling between the left and right barriers. Assuming the junctions are symmetrical and the leads are made of the same FM material, we have $\xi_L = \xi_R = 1$ and $p_L = p_R = p$. The retarded Green's function $\mathbf{G}^r(\epsilon)$ in the current formula of Eq. (5) is also a (4×4) matrix, which can be solved via the standard equation of motion technique[35], which yield the following Dyson's equation

$$\mathbf{G}^r(\epsilon) = \mathbf{G}^{r,0}(\epsilon) + \mathbf{G}^{r,0}(\epsilon)(\mathbf{\Sigma}^{r(L)} + \mathbf{\Sigma}^{r(R)} + \mathbf{V}_c)\mathbf{G}^r(\epsilon). \tag{6}$$

$G^{r,0}(\epsilon)$ describes the edge states of the topological insulator in the absence of TI-lead and inter-edge tunneling couplings, i.e.,

$$G^{r,0}(\epsilon) = \begin{pmatrix} \frac{1}{(\epsilon - vk_0\eta_V + i\eta)} & 0 & 0 & 0 \\ 0 & \frac{1}{(\epsilon + vk_0\eta_V + i\eta)} & 0 & 0 \\ 0 & 0 & \frac{1}{(\epsilon + vk_0\eta_V + i\eta)} & 0 \\ 0 & 0 & 0 & \frac{1}{(\epsilon - vk_0\eta_V + i\eta)} \end{pmatrix}, \tag{7}$$

where k_0 denotes the wavevector associated with the Fermi energy, $V = (\mu_L - \mu_R)$ is the bias voltage and $\eta_V = \pm 1$ is adopted to describe the helical property of the edge channels. $\mathbf{\Sigma}^{r/a(\alpha)} = (\mp i/2)\mathbf{\Gamma}_\alpha(\epsilon)$ are the self-energies due to the lead α, while the matrix $\mathbf{V}_c$ denotes the self-energy due to inter-edge tunneling, and is explicitly given by

$$\mathbf{V}_c = \begin{pmatrix} 0 & 0 & V_{c1} & V_{c2} \\ 0 & 0 & -V_{c2} & V_{c1} \\ V_{c1} & -V_{c2} & 0 & 0 \\ V_{c2} & V_{c1} & 0 & 0 \end{pmatrix}. \tag{8}$$

Finally, the lesser Green's function $\mathbf{G}^<$ in Eq. (5) can be calculated using the Keldysh equation: $\mathbf{G}^<(\epsilon) = \mathbf{G}^r(\epsilon)(\mathbf{\Sigma}^{<(L)} + \mathbf{\Sigma}^{<(R)})\mathbf{G}^a(\epsilon)$, with the scattering function being given by $\mathbf{\Sigma}^{<(\alpha)} = if_\alpha\mathbf{\Gamma}_\alpha$. After solving for the charge current J_α, the differential conductance G_d can be calculated straightly, $G_d = dJ/dV$ with $J_L = -J_R = J$. Accordingly, the tunneling magnetoresistance (TMR) can be derived by the ratio $(G_d(0) - G_d(\theta))/G_d(\theta)$ with $G_d(\theta)$ denoting the conductance associated with the angle θ of the right lead's magnetization.

III. NUMERICAL CALCULATION

In this section, we numerically investigate the transport property of the TI-based device. We adopt the parameters of HgTe quantum wells given in Ref. [6], i.e., with thickness $d = 7$nm, $A = 364.5$meV nm, $B = -686$meV nm^2, $M = -10$meV, and $D = 512$meV nm^2, while the edge state velocity is $v \simeq 5.5\times 10^5$ m/s. The width of the device is set at $W = 1000$nm so that the energy gap of edge states is very tiny and can be neglected[25]. The pinching of the two edge states results in a local modification of the spin-orbit coupling, which may induce spin-conserving and spin-flip tunneling at this narrow region[4,32,33]. We adopt the two phe-

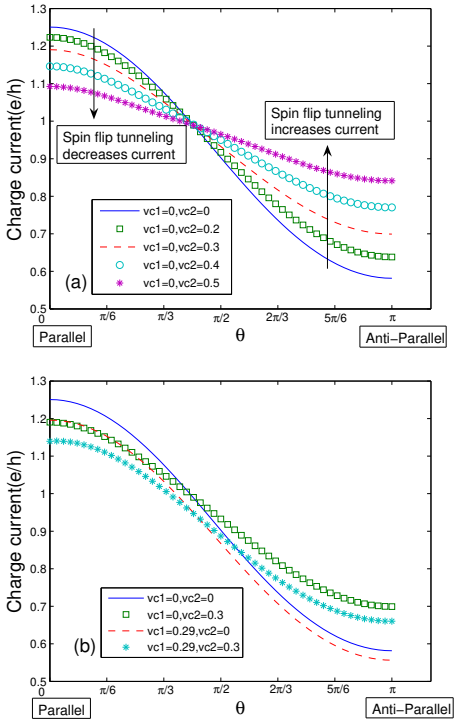

FIG. 2. (a) and (b) Charge current J as a function of the angle θ under different inter-edge tunnel coupling conditions. In (a), we analyze the role of the spin-flip inter-edge coupling, characterized by V_{c2}, while in (b) we consider the effect of spin-conserving inter-edge coupling, characterized by V_{c1}. Other parameters are $\Gamma_0 = 1$, $T = 0.2$, $p = 0.8$, $\mu_0 = 0.3$ and $V = 0.5$.

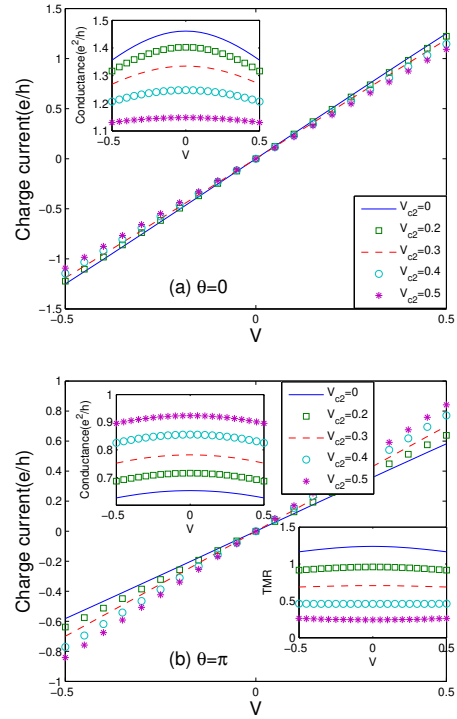

FIG. 3. Bias dependence of the charge current for the cases (a) $\theta = 0$, (b) $\theta = \pi$. The upper insets in (a) and (b) show the bias dependence of the differential conductance, while the lower inset in (b) is the corresponding plot of the TMR. $V_{c1} = 0$ and the other parameters are the same as those of Fig. 2.

nomenological parameters V_{c1} and V_{c2} to describe the two tunneling processes and their relative amplitudes. The Dirac point at equilibrium is set at energy $E = 0$, while the Fermi energy is at $\mu_0 = vk_0 = 0.3\Gamma_0$ ($\Gamma_0 = 10$meV). A bias voltage V is applied to the device, such that the chemical potentials of the leads are $\mu_L = \mu_0 + V/2$ and $\mu_R = \mu_0 - V/2$.

We first analyze the band dispersion of the edge states in the presence of the inter-edge tunneling couplings. From the Hamiltonian H_C of a topological insulator, the energies of top-edge states are given by $E_\sigma = \pm vk$ in the absence of inter-edge tunneling couplings. Once the split-gate voltage V_g is applied and inter-edge tunnel coupling becomes finite, the energies of the edge states are modified to

$$E'_\sigma = \pm\sqrt{(vk + V_{c2})^2 + V_{c1}^2}. \tag{9}$$

The energies of the bottom-edge states can be calculated using the same method. The spin-preserving part of the inter-edge tunnel couplings causes a band gap opening of $\Delta = 2V_{c1}$. Thus electrons cannot flow through the device if the Fermi energy is adjusted to lie within the energy range of $|\mu_0| < V_{c1}$. In this paper, however, we focus on the transport property of the TI-based device in the regime of $|\mu_0| > V_{c1}$, where there exists current flow. We initially study the effect of the inter-edge tunnel coupling on the charge current. Fig. 2(a) shows the effect of the spin-flip tunneling, characterized by the coefficient V_{c2} on the charge current as a function of magnetization orientation θ. The charge current decreases with increasing tunneling strength V_{c2} when $\theta < 5\pi/12$, especially at $\theta = 0$ [the parallel configuration]. However, there occurs an opposite trend, i.e., the charge current can increase with increasing V_{c2} when $\theta > 5\pi/12$. This is especially so when $\theta = \pi$ [the anti-parallel configuration]. The observed trend can be explained by considering the spin-state of electrons in the edge states. In the parallel configuration, spin polarized electrons can flow through the central TI region along one of the edge channels in the absence of the inter-edge coupling. For instance, in the schematic diagram of Fig. 1, we find that when the magnetization of the leads are pointing in the z-direction, then most of the forward electron flux will flow in the top edge state. In the presence of inter-edge spin-flip coupling, however, some of the forward moving electrons in the upper edge will be scattered to the spin-down state in the lower edge. They will encounter a higher probability of being blocked at the right electrode since they are a minority carrier there. On the contrary, for the anti-parallel case, the current is suppressed in the absence of

the inter-edge coupling. Referring to Figure 1 again, let us assume that the magnetization of the left (right) leads are magnetized in the $+z$ ($-z$) direction. The forward spin-up flux in the top edge will be blocked at the right electrode as spin-up electrons are minority carriers there. The presence of inter-edge spin-flip coupling (i.e., finite V_{c2}) enables the spin-up electron in the top edge to be scattered into the forward moving spin-down state in the lower edge. The spin-down electron will have a higher transmission into the right electrode as it will be a majority carrier in that electrode. Thus, by utilizing the presence of spin-flip tunneling at the QPC, one can modulate the transport properties of this TI-based device for different magnetization configurations.

At the same time, the spin-conserving inter-edge tunneling coupling at the QPC induces the back-scattering process. Since this can coexist with the spin-flip tunneling term, it is deservable to investigate the combined effect of these two terms on the charge current, as shown in Fig. 2(b). When there exists only the spin-conserving tunneling, for example $V_{c1} = 0.3$ and $V_{c2} = 0$ [red dashed line], the charge current is decreased by the tunneling term via the back-scattering process. In other words, some of the forward moving electrons in the upper edge will be scattered to the backward moving spin-up states in the lower edge, thus decreasing the overall charge current. The reduction in current due to the back-scattering is greater for the parallel configuration than that for the antiparallel case. This is because the current reduction in the parallel case is mainly due to the back-scattering of majority spin carriers, and this involves more electrons than that of minority electrons in the anti-parallel case.

In the presence of both types of inter-edge tunnel coupling, i.e. both the spin-flip and spin-conserving types, the net result will be suppression (enhancement) of charge current when the device is in the parallel (antiparallel) configuration. In the parallel configuration, both the spin-flip and spin-conserving tunneling reduce the current, the former by scattering to the minority spin state, while the latter by backscattering. However, in the antiparallel configuration, the two inter-edge couplings have opposite effects − the spin-flip (spin-conserving) process increases (decreases) the current. When the two are of equal strength, e.g., $V_{c1} = V_{c2} = 0.3$, the spin-flip process dominates, and so there is a net increase in current in the antiparallel configuration [see Fig. 2(b)]. The current suppression due to the spin-conserving tunneling also results in the cross-over between net enhancement and net suppression of charge current occurring at a large-angle configuration beyond $\theta = 5\pi/12$ [see Fig. 2(b)]. Thus, the transport properties of our TI-based device can be effectively modulated by adjusting the relative strengths of the two types of inter-edge tunneling couplings across the QPC. In order to experimentally verify the above results, one must first prepare the HgTe-based device with transverse width of at least $W = 1000$ nm, as schematically shown in Fig. 1. For the two ferromagnetic leads, the magnetization of the left lead is fixed and pointed in the out-of-plane $\hat{\mathbf{z}}$ direction, while the right lead is made of a softer magnetic material, so that its magnetization direction can be changed from $\theta = 0$ to $\theta = \pi$ with respect to the left lead, by application of a magnetic field. One can modulate the width of the QPC by using the gate voltage V_g, which would in turn induce different tunneling strengths V_{c1} and V_{c2}, due to the finite overlap between edge states on the upper and the lower sides[33]. By analyzing the voltage dependence of the charge current, one may determine the variation of the charge current as a function of V_{c1} and V_{c2}.

Next, we analyze the charge current J and the conductance G_d of the TI-based device under varying bias voltage. In Fig. 3(a) and (b), the bias dependence of J is plotted for different spin-flip coupling strengths V_{c2}, for the parallel ($\theta = 0$), and antiparallel ($\theta = \pi$) configurations. As noted earlier, for the parallel (antiparallel) configuration, J decreases (increases) as V_{c2} increases. Similarly, the bias dependence plot of G_d also shows a decrease (increase) with increasing V_{c2} when $\theta = 0$ ($\theta = \pi$), as shown in the upper insets of Fig. 3(a) [(b)]. This may be explained by the fact that a finite V_{c2} would lead to coupling of two edge states with opposite spins, resulting in spin mixing and thus reducing the degree of spin asymmetry in the device. Consequently, the TMR ratio decreases with increasing V_{c2}, as shown by the lower inset of Fig. 3(b). For both configurations, the conductance also decreases with increasing bias voltage V, with a larger decrease occurring for the parallel case. This translates to a slight decrease in TMR ratio with bias voltage V for small coupling strength V_{c2}. Hence, the conductance and the TMR of the TI-based device can be modulated by both the source-drain voltage V, and the split-gate voltage V_g, which alters the coupling strength V_{c2}.

IV. CONCLUSION

In summary, we have investigated the transport of a two-dimensional topological insulator (TI) sandwiched between two ferromagnetic (FM) leads, and incorporating a quantum point contact (QPC) which couples the edge states along the top and bottom boundaries. The conductance across the device is calculated via the nonequilibrium Green's function (NEGF) method. We found that spin-flip tunnel coupling between the edge states mediated by the QPC can enhance (suppress) the current when the magnetization of the two FM leads is in the antiparallel (parallel) configuration. On the other hand, the spin-conserving tunnel coupling leads to backscattering which reduces the overall current regardless of the magnetization alignment of the FM leads. The conductance and TMR of the TI-based device can be controlled by both the source-drain voltage V, as well as the split-gate voltage V_g, the latter modifying the inter-edge coupling strengths across the QPC. Our proposed device

suggests a new class of TI-based devices which incorporate a QPC to electrically control the inter-edge coupling, so as to harness the topological and spin-polarized nature of the TI edge states for practical application.

ACKNOWLEDGMENTS

We greatfully acknowledge the National University of Singapore (NUS) Grant No. R-263-000-632-592 and the SMF-NUS Research Horizons Award for financially supporting their work. The work was also supported by Innovation Research Team for Spintronic Materials and Devices of Zhejiang Province.

[1] C. L. Kane and E. J. Mele, Phys. Rev. Lett. **95**, 146802 (2005).
[2] B. A. Bernevig and S. C. Zhang, Phys. Rev. Lett. **96**, 106802 (2006).
[3] D. Hsieh, D. Qian, L. Wray, Y. Xia, Y. S. Hor, R. J. Cava, and M. Z. Hasan, Nature **452**, 970 (2008).
[4] H. J. Zhang, C. Liu, X. Qi, X. Dai, Z. Fang, and S. Zhang, Nature Phys. **5**, 438 (2009).
[5] Y. Xia, D. Qian, D. Hsieh, L. Wray, A. Pal, H. Lin, A. Bansil, D. Grauer, Y. S. Hor, and R. J. Cava, Nature Phys. **5**, 398 (2009).
[6] X. L. Qi and S. C. Zhang, Rev. Mod. Phys. **83**, 1057 (2011).
[7] M. Z. Hossain, S. L. Rumyantsev, K. M. F. Shahil, D. Teweldebrhan, M. Shur, and A. A. Balandin, ACS Nano 5, 2657 (2011).
[8] K. M. F. Shahil, M. Z. Hossain, D. Teweldebrhan, and A. A. Balandina, Appl. Phys. Lett. **96**, 153103 (2010).
[9] T. Fujita, M. B. A. Jalil, and S. G. Tan, Appl. Phys. Express **4**, 094201 (2011).
[10] J. E. Moore, Nature 464, 194 (2010).
[11] H. Tang, D. Liang, R. L. J. Qiu, and X. P. A. Gao, ACS Nano **5**, 7510 (2011).
[12] D. Teweldebrhan, V. Goyal, and A. A. Balandin, Nano Lett. **10**, 1209 (2010).
[13] D. Teweldebrhan, V. Goyal, M. Rahman, and A. A. Balandin, Appl. Phys. Lett. **96**, 053107 (2010).
[14] V. Goyal, D. Teweldebrhan, and A. A. Balandina, Appl. Phys. Lett. **97**, 133117 (2010).
[15] B. A. Bernevig, T. L. Hughes, and S. C. Zhang, Science **314**, 1757 (2006).
[16] M. Konig, S. Wiedmann, C. Brune, A. Roth, H. Buhmann, L. W. Molenkamp, X. L. Qi, and S. C. Zhang, Science **318**, 766 (2007).
[17] A. Roth, C. Brüne, H. Buhmann, L. W. Molenkamp, J. Maciejko, X. L. Qi, and S. C. Zhang, Science **330**, 1746 (2009).
[18] M. Buttiker, Science **325**, 278 (2009).
[19] L. Fu and C. L. Kane, Phys. Rev. B **76**, 045302 (2007).
[20] S. Murakami, Phys. Rev. Lett. **97**, 236805 (2006).
[21] C. X. Liu, T. L. Hughes, X. L. Qi, K. Wang, and S. C. Zhang, Phys. Rev. Lett. **100**, 236601 (2008).
[22] I. Knez, R. R. Du, and G. Sullivan, Phys. Rev. B **81**, 201301(R) (2010).
[23] A. Shitade, H. Katsura, J. Kuneš, X. L. Qi, S. C. Zhang, and N. Nagaosa, Phys. Rev. Lett. **102**, 256403 (2009).
[24] M. Wada, S. Murakami, F. Freimuth and G. Bihlmayer, Phys. Rev. B **83**, 121310(R) (2011).
[25] B. Zhou, H. Z. Lu, R. L. Chu, S. Q. Shen, and Q. Niu, Phys. Rev. Lett. 101, 246807 (2008).
[26] C.Y. Hou, E.A. Kim, and C. Chamon, Phys. Rev. Lett. **102**, 076602 (2009).
[27] A. Strom, and H. Johannesson, Phys. Rev. Lett. **102**, 096806 (2009).
[28] Y. Tanaka, and N. Nagaosa, Phys. Rev. Lett. **103**, 166403 (2009).
[29] J. C. Y. Teo, and C. L. Kane, Phys. Rev. B **79**, 235321 (2009).
[30] V. A. Zyuzin, and G. A. Fiete, Phys. Rev. B **82**, 113305 (2010).
[31] L. B. Zhang, F. Cheng, F. Zhai, and K. Chang, Phys. Rev. B **83**, 081402 (2011).
[32] F. Dolcini, Phys. Rev. B **83**, 165304 (2011).
[33] V. Krueckl and K. Richter, Phys. Rev. Lett. 107, 086803 (2011).
[34] J. Maciejko, E. A. Kim, and X. L. Qi, Phys. Rev. B **82**, 195409 (2010).
[35] Y. Meir and N. S. Wingreen, Phys. Rev. Lett. **68**, 2512 (1992); A. P. Jauho, N. S. Wingreen, and Y. Meir, Phys. Rev. B **50**, 5528 (1994).